

Research article

Fahime Ghashghaei, Alireza Rashedi, Farrokh Sarreshtedari* and Mahmood Sabooni

Effect of the magnetically induced dichroism on the distribution of atomic polarization in Cesium vapor cells

<https://doi.org/10.1515/aot-2019-0066>

Received September 8, 2019; accepted June 1, 2020; published online July 14, 2020

Abstract: Distribution of the atomic polarization in a Cesium vapor cell, induced by optical pumping, is analytically calculated and discussed when an external magnetic field interacts with the system. Based on the rate equations of the optically pumped atomic system and considering the effect of magnetically induced dichroism on the absorption of polarized propagating light, we have obtained the light intensity and atomic polarization distribution along the propagation direction of the gas cell. It is shown that based on the initial light polarization and the laser detuning, the external magnetic field considerably changes the polarization distribution. The obtained results of the polarization distribution versus applied magnetic field can be used for different investigations, including the study of the atomic magnetometer's sensitivity.

Keywords: distribution of atomic polarization; magnetically induced dichroism; optically pumped alkali atoms.

1 Introduction

Many different atomic experiments incorporate optically polarized alkali atoms as the quantum system of the light-matter interaction. Atomic magnetometers, optical rotation experiments, and alkali lasers are some experiments which involve the evolution of the atomic

polarization [1–3]. In atomic magnetometers which incorporate optically detected magnetic resonance (ODMR), the detection process strongly depends on the population imbalance of the Zeeman sublevels, which result in a net atomic polarization. Therefore, calculating and engineering of the atomic polarization distribution and its evolution in the alkali vapor cells is significantly important and is considered in different works [4–10]. In this regard, when a circularly polarized light illuminates the atomic vapor cell, in the absence of an external magnetic field in which the Zeeman sublevels are all degenerate, the atomic absorption is the same for both right and left circular polarization. However, when the magnetic field is introduced, because of the magnetically induced dichroism, the atomic absorption would be different for right and left circularly polarized lights, which also changes the population of the Zeeman sublevels. Here we have analytically discussed the effect of magnetically induced dichroism on the distribution of the atomic polarization in a Cesium vapor cell. We have incorporated the rate equations (and also the notations) discussed in the study by Lang et al [8] in the calculation of the sublevel populations in the presence of laser pumping and external fields. Furthermore, the considered parameters in the calculations are based on the experimental setup we have used for investigation of the magnetically induced dichroism in a Cesium vapor cell pumped by an external cavity diode laser [11, 12].

2 Theoretical model

Cesium atom has a hydrogen-like level structure $[\text{Xe}]6s^1$, which contains a single outer-shell electron. In the ground state, because of the electron spin and zero orbital angular momentum, the total angular momentum is equal to $J = 1/2$. For the first excited state ($L = 1$), the total angular momentum equals to $J = 1/2$ or $J = 3/2$. Thus, there are two transition lines, among which, the transition from $6^2S_{1/2} \rightarrow 6^2P_{1/2}$ is called the D_1 line, which is considered in this work [11]. With the ground-state nuclear spin of $I = 7/2$, the hyperfine interaction splits the $6S_{1/2}$ ground state into the two hyperfine levels of $F = 3, 4$ and

*Corresponding author: Farrokh Sarreshtedari, Magnetic Resonance Research Laboratory, Department of Physics, College of Science, University of Tehran, 1439955961, Tehran, Iran, E-mail: f.sarreshtedari@ut.ac.ir

Fahime Ghashghaei and Alireza Rashedi: Magnetic Resonance Research Laboratory, Department of Physics, College of Science, University of Tehran, 1439955961, Tehran, Iran

Mahmood Sabooni: Department of Physics, College of Science, University of Tehran, 1439955961, Tehran, Iran; Institute for Quantum Computing, Department of Physics and Astronomy, Waterloo, Ontario, N2L3G1, Canada

the lowest excited state, $6P_{1/2}$ splits into the hyperfine levels of $f = 3, 4$ [13]. Each of these hyperfine levels has $2F + 1$ Zeeman sublevels which are degenerate in the absence of an external magnetic field. At thermal equilibrium, the distribution of different Zeeman sublevels obeys Boltzmann thermal distribution. However, when circularly polarized laser light illuminates the Cesium vapor cell, the distribution becomes substantially different. The rate equations which describe the population evolution of the 16 ground-state sublevels and 16 excited-state sublevels under the influence of circularly polarized pumping field is given by Eq. (1):

$$\begin{cases} \dot{p}_{F,M} = -\Gamma_p^{F,M,f,m} p_{F,M} \\ \quad + \sum_{f,m} \Gamma_{spont}^{f,m,F,M} p_{f,m} \\ \quad - \gamma_1 (p_{F,M} - p_{F,M}^{(0)}) \\ \dot{p}_{f,m} = + \sum_{F,M} \Gamma_p^{F,M,f,m} p_{F,M} - \Gamma_{spont}^{tot} p_{f,m} \end{cases} \quad (1)$$

In these equations, $\Gamma_p^{F,M,f,m}$ is the transition rate from $|F, M\rangle$ to $|f, M+1\rangle$, $\Gamma_{spont}^{f,m,F,M}$ is the spontaneous emission rate from $|f, m\rangle$ to $|F, M\rangle$, and $\Gamma_{spont}^{tot} = \sum_{F',M'} \Gamma_{spont}^{f,m,F',M'}$ is the total spontaneous emission rate. γ_1 is the isotropic relaxation rate of the ground-state populations, and the quantities $p_{F,M}^{(0)}$ are the ground-state populations in thermal equilibrium:

$$\begin{cases} p_{F=3,M}^{(0)} = \frac{1}{7 + 9 \exp\left(-\frac{h\nu_{hfs}}{KT}\right)} \\ p_{F=4,M}^{(0)} = \frac{1}{9 + 7 \exp\left(\frac{h\nu_{hfs}}{KT}\right)} \end{cases} \quad (2)$$

In Eq. (2), h is the Plank constant, ν_{hfs} is the Cesium ground-state hyperfine splitting, and K is the Boltzmann constant. It should be noted that in the derivation of Eq. (1), it is assumed that the laser linewidth is high enough that the ground-state and excited-state hyperfine splitting could not be resolved in the optical spectra. Following the approach discussed in the study by Lang et al [8], Eq. (1) can be simplified by neglecting the fast-transient processes in the excited state ($p_{f,m} = 0$). Therefore, the rate equation for the probability of the ground-state sublevels can be derived as follows:

$$\begin{aligned} \dot{p}_{F,M} = & -\gamma_p \sum_f \mathfrak{R}_{F,M,f,m+q} p_{F,M} + \gamma_p (2j+1) \\ & \times \sum_{F',M'} p_{F',M'} \mathfrak{R}_{F',M',f,m'+q} \mathfrak{R}_{f,M'+q,F,M} \\ & - \gamma_1 (p_{F,M} - p_{F,M}^{(0)}) \end{aligned} \quad (3)$$

where γ_p is the optical pumping rate; $q = 0, +1$, and -1 for linear, right, or left circularly polarized light, respectively; and the $\mathfrak{R}_{F,M,f,m}$ is defined as follows using the Wigner 6j-symbols.

$$\begin{aligned} \mathfrak{R}_{F,M,f,m} = & (2F+1)(2f+1) \\ & \times \begin{pmatrix} f & 1 & F \\ -m & m-M & M \end{pmatrix}^2 \times \left\{ \begin{matrix} j & f & I \\ F & J & 1 \end{matrix} \right\}^2 \end{aligned} \quad (4)$$

The first term in Eq. (3) describes the rate of depopulation from $|F, M\rangle \rightarrow |f, M+q\rangle$, according to the input laser polarization. The second term describes the rate at which the population at each arbitrary ground state $|F', M'\rangle$ goes to $|f, M'\rangle$ and returns back to $|F, M\rangle$. The last term describes the population relaxation rate to its equilibrium value. It is worth mentioning that for a light composed of the right and left circular polarization, based on the ratio of the polarization, the optical pumping rate (γ_p) is different for each of them. When the atomic polarization in the excited state is totally destroyed, the optical pumping process is referred as “depopulation.” On the other hand, the term “repopulation” is used whenever the atomic polarization in the excited state is totally preserved [8, 14]. It should be noted that the dominant *repopulation* pumping regime is considered in development of the mentioned rate equations. Eq. (3) is a system of the differential equation which can be described as follows:

$$\frac{d\vec{P}}{dt} = W\vec{P} + \vec{P}_0 \quad (5)$$

where P is an array with 16 elements according to the population of 16 different ground-state sublevels, W is a pumping-relaxation (16×16) matrix that describes the relation of each sublevel population rate to all other ground-state populations, and P_0 is the equilibrium population of 16 sublevels, which can be calculated from Eq. (2). Development of the matrix W requires checking all the possible transitions based on the input light polarization and then calculating their transition rates according to Eq. (3). We have constructed W , and then the differential Eq. (5) is numerically solved. In the appendix, it has been shown that the summation of all elements in each column of matrix W should be equal to -1 . Checking these criteria has also confirmed the correctness of our calculation for the development of the pumping-relaxation matrix W .

It should also be noted that Eq. (3) depends on discrete values of $q = 0, +1, -1$ for linearly polarized, right circularly polarized, and left circularly polarized light. In this regard, for considering the effect of the light

polarization on the distribution of populations, following the approach of Lang et al [8], after the calculation using $q = +1$ and -1 , based on the ratio of the right and left circularly polarization, the averaged value of $p_{F, M}$ is obtained using Eq. (6).

$$p_{F, M} = \frac{1 + \zeta_{\text{pol}}}{2} p_{F, M}(\sigma_+) + \frac{1 - \zeta_{\text{pol}}}{2} p_{F, M}(\sigma_-) \quad (6)$$

In Eq. (6), ζ_{pol} is a parameter in the range of ± 1 , which describes the degree of circular polarization of the pumping light. The value of $\zeta_{\text{pol}} = 0$ describes the linearly polarized light, while $\zeta_{\text{pol}=\pm 1}$ corresponds to right/left (σ_{\pm}) circularly polarized light, respectively.

We have numerically solved Eq. (3) for obtaining the populations of different Zeeman sublevels for a desired polarized pumping light. The nonuniform distribution of the populations causes the polarization of the atoms, which is defined as follows:

$$F_i = \langle F_Z \rangle_i = \frac{1}{M} \sum_M p_{i, M} M \quad (7)$$

The absorption of light through the cell is a function of different parameters, including the atomic vapor properties, polarization of the incident light, and also the polarization of atoms at each location in the cell. On the other hand, the absorption of light changes the pumping rate, which is an essential factor in determining the atomic polarization. Here we have numerically calculated the distribution of the atomic polarization as the light travels through the vapor cell. We have also included the effect of an externally applied magnetic field, which induces magnetic dichroism and changes the frequency dependence of the light absorption for right and left circularly polarized lights.

3 Experimental setup

In experiments in which the atomic vapor cell is placed under an external magnetic field, the application of the magnetic field splits the absorption profile for the σ_{\pm} light polarizations.

A schematic of the experimental setup for investigating the dependence of this splitting to the applied magnetic field is shown in Figure 1. The setup includes an Extended Cavity Diode Laser (ECDL) source, which is tuned on the D_1 absorption line of the Cesium [11], a Cesium spectroscopic cell, two polarizing beam splitters (PBS), a quarter wave plate ($\lambda/4$), and two photo detectors (PD). When the magnetic field is zero, the absorption lines for the right (σ_+) and left (σ_-) circularly polarized lights are identical. While in the

presence of the magnetic field, it will be split in frequency [15]. Figure 1 (inset) shows the mentioned results for the absorption profiles of σ_+ and σ_- circularly polarized input light. This figure (with a vertical scale of 2 V/Div for σ_+ and σ_- traces) shows the experimental absorption in the presence of a magnetic field (-80 G) in the light propagation direction. The splitting of the absorption lines is about $\Delta f = 180$ MHz, which is about 0.6 times of Cesium linewidth at the room temperature (Full width at half maximum). It should be noted that for better representation, we have intentionally changed the gains of the two photodiodes amplifiers. This is the reason that with no magnetic field, although the center wavelengths of σ_+ and σ_- absorption lines are the same, their amplitudes are different.

4 Results and discussion

The atomic polarization for the desired hyperfine level is obtained by solving the rate equation [Eq. (3)] using Eq. (6). Figure 2a and b show the calculated time evolution of the atomic polarization for ground-state hyperfine level of $F = 4$ ($F = 3$) as the light illuminate the atomic system, respectively.

Figure 2 shows the results for constant pumping rate and different degrees of circular polarization of the pumping beam ζ_{pol} . It should be noted that the time scale is normalized by the inverse of the ground-state relaxation rate (γ_1^{-1}). Figure 3 shows the calculated time evolution of

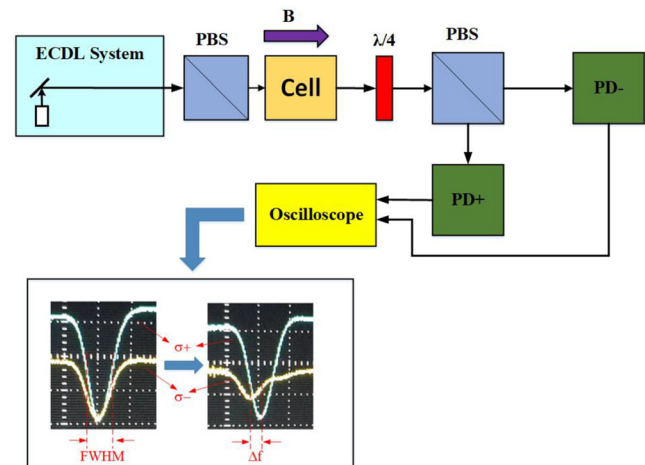


Figure 1: Schematic of the experimental setup. The setup includes an Extended Cavity Diode Laser (ECDL) source which is tuned on the D_1 absorption line of the Cesium, a Cesium spectroscopic cell, two polarizing beam splitters (PBS), a quarter wave plate ($\lambda/4$), and two photo detectors (PD). Inset: the absorption profiles for the σ_+ and σ_- circularly polarized input lights in the absence (left signals) and presence of external magnetic field (right signals).

the atomic polarization for the ground-state hyperfine level of $F = 4$ for different normalized pumping rate γ_p/γ_1 while the degree of the circular polarization is $\xi_{\text{pol}} = 0.8$.

When the incident beam propagates through the cell, based on the light polarization and also the atomic polarization, it becomes partially or wholly absorbed by the Cesium vapor. This light absorption and also the difference between the attenuation of right and left circularly polarized light are important parameters for determining the polarization distribution along the propagation direction. As shown in Figure 1 (inset), because of the magnetically induced dichroism, there is splitting between the absorption profiles of the right and left circularly polarized light. In the presence of the external magnetic field, at each specific detuning, there is a difference between the attenuation of the two polarized lights. This difference would be

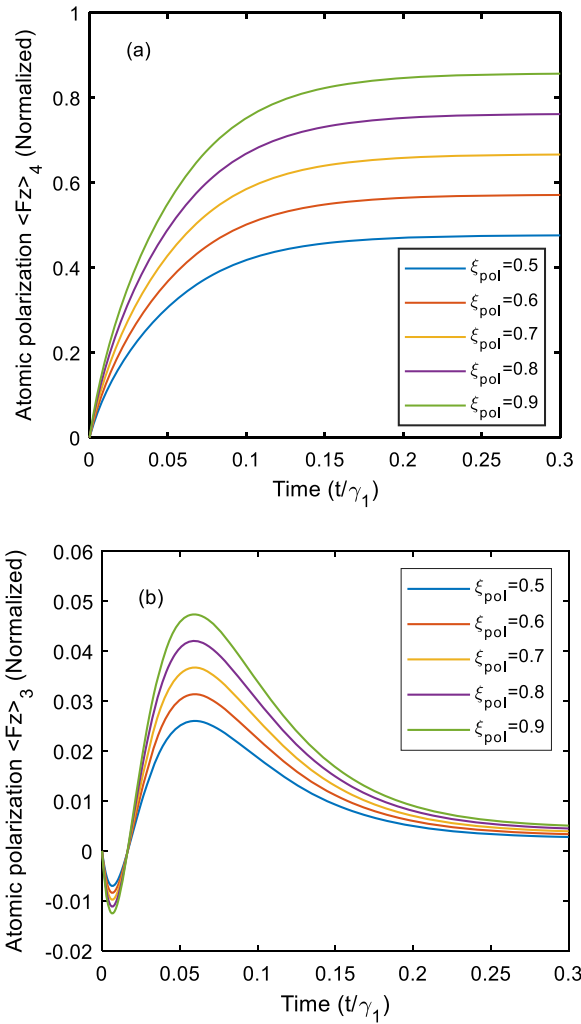


Figure 2: The time evolution of the hyperfine polarization (F_n) under repopulation pumping for different degrees of circular polarization (ξ_{pol}) at the normalized pump rate of $\gamma_p/\gamma_1 = 700$. (a) $F = 4$ and (b) $F = 3$.

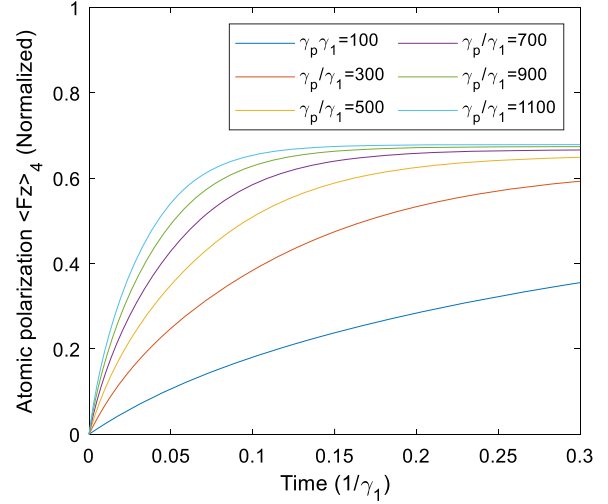


Figure 3: The time evolution of the hyperfine polarization $F_4 = \langle F_z \rangle_4$ for different normalized pump rates $\gamma_p/\gamma_1 = 100, 300, 500, 700, 900,$ and 1100 while the degree of circular polarization is $\xi_{\text{pol}} = 0.8$.

increased if the applied magnetic field increases. Considering the atomic polarization inside the cell, the light intensity along the propagation direction is related to the light and atomic polarization as Eq. (8) [16]:

$$\frac{d}{dz} I = -n\sigma(v)I(1 - 2\xi_{\text{pol}}\langle F_z \rangle) \quad (8)$$

where I is the light intensity, n is the density of the alkali vapor, $\sigma(v)$ is the absorption cross section, z is the position in the cell, ξ_{pol} is the degree of circular polarization, and $\langle F_z \rangle$ is the total atomic polarization, that is, the average value of the atomic polarization of the two ground-state levels $1/2(\langle F_{z>4} + \langle F_{z>3})$. For linearly polarized light ($\xi_{\text{pol}} = 0$), the solution is an exponential attenuation; however, for a nonzero ξ_{pol} , the calculation of the intensity Eq. (8) and atomic polarization Eq. (7) is a coupled problem which should be simultaneously computed. Figure 4a shows the obtained result for the calculation of the polarization distribution through a 10-cm length cell for different degrees of circular polarization of the pumping beam (ξ_{pol}). Figure 4b shows the result of the same calculation for obtaining the light intensity through the vapor cell.

It is evident that for a linearly polarized light ($\xi_{\text{pol}} = 0$), there is not any atomic polarization, while by increasing the ξ_{pol} , more atomic polarization is developed. Furthermore, as the light travels along the cell, the polarization decreases. That is obviously because of the light absorption, which decreases the pumping rate. For a better representation of the atomic polarization and light intensity distribution inside the Cesium vapor cell, Figure 5 shows these values when the ξ_{pol} is swept from -1 to 1 .

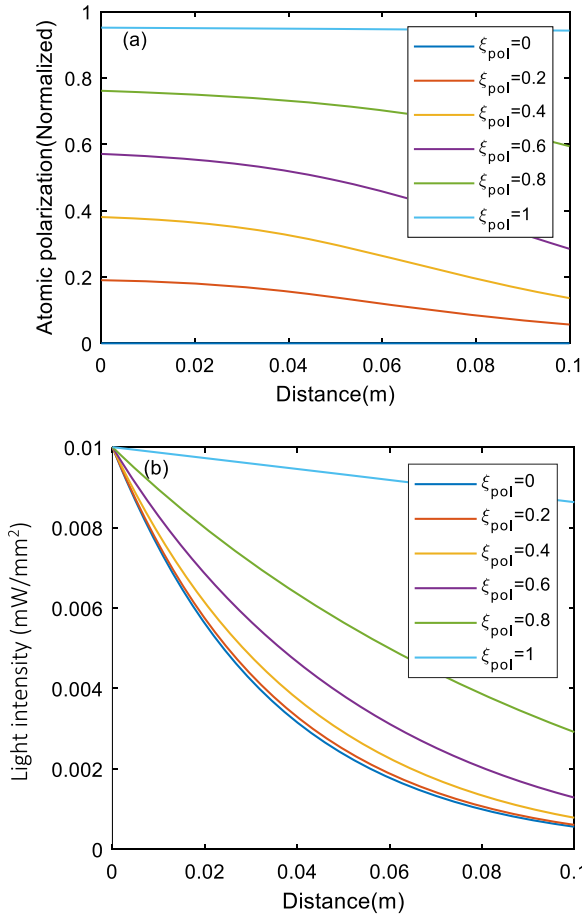


Figure 4: (Color online) (a) Polarization distribution and (b) distribution of the light intensity inside the Cesium vapor cell for different degrees of circular polarization (ξ_{pol}). For both cases: $\gamma_p/\gamma_1 = 700$, $n = 10^{13} \text{ cm}^{-1}$, $I_0 = 10 \text{ mW/mm}^2$.

Until now, the discussed results were without considering the effect of the external magnetic field on population distribution. As the linearly polarized light is composed of the right and left circularly polarized components, when the magnetic field is applied to the vapor cell, the difference between the attenuation of two circular polarizations changes the normal distribution of the atomic polarization and also the light intensity inside the cell. The distribution of the atomic polarization and laser intensity along the propagation direction has been calculated when, due to the external magnetic field, the center of the absorption frequencies for σ_+ and σ_- incident light is split. As we are mostly interested in small-frequency detuning around the center absorption frequency, we have considered a constant atomic cross section, and also it is assumed that the rate equations do not change by applying the small magnetic field. Furthermore, based on our experimental results, for sufficiently small magnetic fields (where the nonlinear Zeeman effects could be ignored), we have

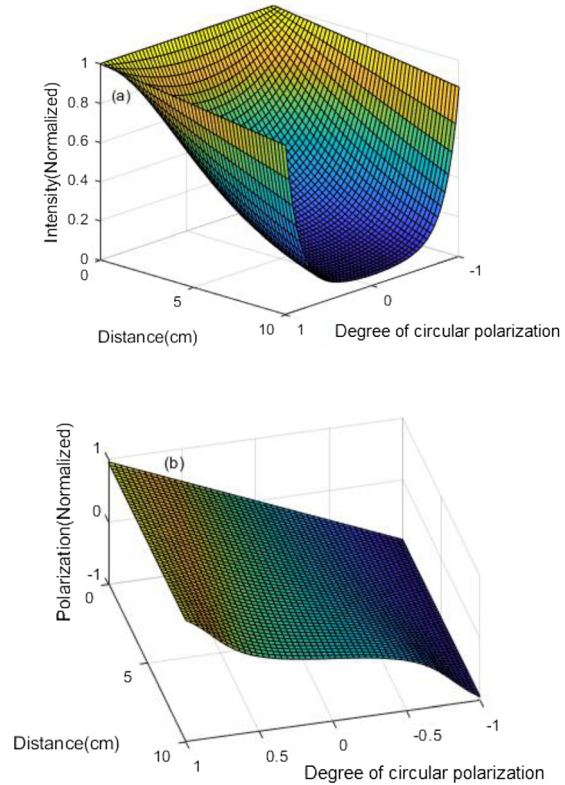


Figure 5: (a) Distribution of the light intensity inside the Cesium vapor cell for different degrees of circular polarization (ξ_{pol}) and (b) polarization distribution. For both cases: $\gamma_p/\gamma_1 = 700$, $n = 10^{13} \text{ cm}^{-1}$.

assumed a linear shift of the absorption lines (for σ_+ and σ_- light polarizations) proportional to the applied magnetic field. Based on these assumptions, we have modeled the effect of the magnetic field by the distribution of the polarization parameter (ξ_{pol}) over frequency detuning. In this model, a fixed magnetic field results in a specific splitting of the σ_+ and σ_- absorption profiles, and so the ratio of the circular polarization (ξ_{pol}) has a nonlinear distribution (proportional to the difference between the σ_+ and σ_- absorption lines) over the frequency detuning. As the applied magnetic field changes, the center wavelengths of σ_+ and σ_- Lorentzian absorption lines change, and so the distribution of the ξ_{pol} over frequency detuning would change. In this regard, starting from the beginning of the cell, for each point through the path of the light, we have simultaneously calculated Eqs. (5) and (8) for obtaining the atomic polarization and also the light intensity. Figure 6 shows the dependence of the light intensity and atomic polarization distribution on the laser detuning. In this simulation, it is assumed that the incident light to the face of the cell is linearly polarized, and the normalized pumping rate is $\gamma_p/\gamma_1 = 700$. Furthermore, the considered

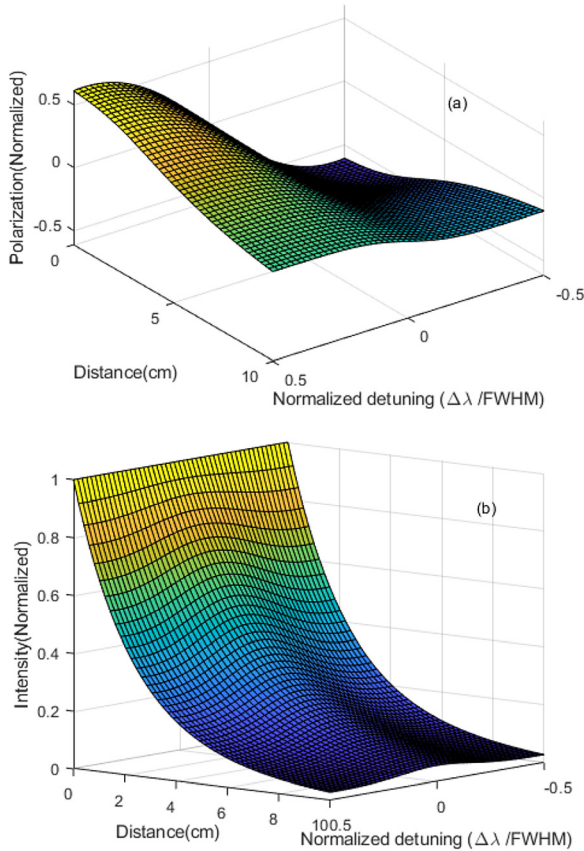


Figure 6: (a) Distribution of the atomic polarization along the vapor cell and (b) the light intensity along the propagation direction versus laser detuning.

splitting between σ_+ and σ_- absorption profiles is $0.6 \cdot \text{FWHM}$, which corresponds to applying a magnetic field of about 80 Gauss to the vapor cell.

As shown in Figure 6b, the intensity has a maximum on the resonant frequency and two minimums around it. This means that at the resonant frequency, the absorption has slightly decreased as the σ_+ and σ_- absorption profiles are shifted by the magnetic field. In this regard, Figure 6b represents a modification of the typical absorption profiles, with the insertion of a small dip on the top of the absorption signal.

5 Conclusion

Here we have analytically investigated the distribution of the atomic polarization inside a Cesium vapor cell. The considered cell is illuminated by a pumping laser source and is placed inside a uniform external magnetic field along the propagation direction. At each position along the cell, the population of Zeeman sublevels, which

determines the atomic polarization, depends on the laser pumping rate. This is while the laser intensity at each point is a function of the light absorption and also the atomic polarization. Furthermore, in the presence of the magnetic field, because of the magnetically induced dichroism, the light absorption inside the cell depends on the light polarization and the value of the magnetic field. In this regard, by considering the system rate equations for calculating the Zeeman sublevel populations and considering the mentioned factors on the light propagation, we have obtained the distribution of the atomic polarization inside the Cesium vapor cell. This calculation method for analyzing the distribution of the atomic polarization could be used in different experiments when the atomic vapor cells are placed in an external magnetic field.

Acknowledgment: The authors would like to thanks the Iran National Science Foundation (INSF) for their support.

Author contribution: All the authors have accepted responsibility for the entire content of this submitted manuscript and approved submission.

Research funding: The research was funded by Iran National Science Foundation (INSF).

Conflict of interest statement: The authors declare no conflicts of interest regarding this article.

Appendix

Ignoring the fast-transient processes in the excited state, the summation probabilities of all ground-state sublevels should be constant and equal to 1. In this regard, considering the evolution of ground-state probabilities by Eq. (5), at each time step, the summation of changes in different sublevel probabilities should be equal to zero.

$$\begin{cases} \sum dp_i = 0 \\ \frac{\Delta \vec{P}}{\Delta t} = W\vec{P} + \vec{P}_0 \end{cases} \quad (\text{A1})$$

Thus, the summation of all elements of WP vector should be equal to -1 . Knowing that $\sum p_i = 1$, the summation of all elements in each column of matrix W should be equal to -1 .

References

- [1] M. Auzinsh, Budker D., Rochester Sm. *Optically Polarized Atoms: Understanding Light-Atom Interactions*. New York: Oxford University Press; 2010.

- [2] D. Budker and M. Romalis, "Optical magnetometry," *Nat. Phys.*, vol. 3, pp. 227–234, 2007.
- [3] G. A. Pitz and M. D. Anderson, "Recent advances in optically pumped alkali lasers," *Appl. Phys. Rev.*, vol. 4, Art no. 041101, 2017.
- [4] D. Budker, W. Gawlik, D. F. Kimball, S. M. Rochester, V. V. Yashchuk, A. Weis "Resonant nonlinear magneto-optical effects in atoms." *Rev. Mod. Phys.* vol. 74, p.74, 2002. 1153.
- [5] J. W. Weis and S. Kanorsky, "Quantitative interpretation of the nonlinear Faraday effect as a Hanle effect of a light-induced birefringence," *J. Optic. Soc. Am. B*, vol. 10, no. 4, pp. 716–724, 1993.
- [6] S. Ulzega, A. Hofer, P. Moroshkin, R. Müller-Siebert, D. Nettels, and A. Weis, "Measurement of the forbidden electric tensor polarizability of Cs atoms trapped in solid He4," *Phys. Rev. A*, vol. 75, Art no. 042505, 2007.
- [7] A. Hatakeyama, K. Enomoto, N. Sugimoto, and T. Yabuzaki, "Atomic alkali-metal gas cells at liquid-helium temperatures: Loading by light-induced atom desorption," *Phys. Rev. A*, vol. 65, Art no. 022904, 2002.
- [8] S. Lang, S. Kanorsky, T. Eichler, R. Muller-Siebert, T. W. Hansch and A. Weis, "Optical pumping of Cs atoms in solid 4He," *Phys. Rev. A*, vol. 60, pp. 3867–3877, 1999.
- [9] V. Schultze, B. Schillig, R. IJsselsteijn, T. Scholtes, S. Woetzel and R Stolz, "An optically pumped magnetometer working in the light-shift dispersed Mz mode," *Sensors (Basel)*, vol. 17, no. 3, pp. 561, 2017.
- [10] T. Scholtes, S. Pustelny, S. Fritzsche, V. Schultze, R. Stolz, and H.-G. Meyer, "Suppression of spin-exchange relaxation in tilted magnetic fields within the geophysical range," *Phys. Rev. A*, vol. 94, Art no. 013403, 2016.
- [11] A. Rashedi, F. Ghashghaei, F. Sarreshtedari M Sabooni, B. Babaei, and S. Golshan Khavas, "Investigation of the magnetically induced dichroism in cesium atomic vapor," in *Annual Physics Conf. of Iran, Tabriz*, August 2019, pp. 26–29confproc.
- [12] A. Rashedi, F. Ghashghaei, F. Sarreshtedari M Sabooni, B. Babaei, and S. Golshan Khavas, 2019, "A highly stable and tunable extended cavity diode laser," in *27th Iranian Conference on Electrical Engineering (ICEE2019), Yazd, Iran*, May 2019, pp. 1–2confproc.
- [13] D. A. Steck, *Cesium D Line Data, Theoretical Division (T-8), MS B285, NM 87545*, Los Alamos National Laboratory Los Alamos, 2003.
- [14] W. Happer, "Optical pumping", *Rev. Mod. Phys.*, vol. 44, pp. 169–250, 1972.
- [15] K. L. Corwin, Z. T. Lu, C. F. Hand, R. J. Epstein, and C. E. Wieman, "Frequency-stabilized diode laser with the Zeeman shift in an atomic vapor", *Appl. Optic.*, vol. 37, pp. 3295–3298, 1998.
- [16] S. Seltzer, "Developments in alkali metal atomic magnetometry," Ph.D. dissertation, Dept. Phys, Princeton Univ, Princeton, 2008.